

# CKM angle $\gamma$ measurements at LHCb

Alexis Vallier

Laboratoire de l'Accélérateur Linéaire, Université Paris-Sud 11, CNRS/IN2P3, Orsay, France.

E-mail: vallier@lal.in2p3.fr

**Abstract.** The CKM angle  $\gamma$  remains the least known parameter of the CKM mixing matrix. The precise measurement of this angle, as a Standard Model benchmark, is a key goal of the LHCb experiment. We present four recent  $CP$  violation studies related to the measurement of  $\gamma$ , including amplitude analysis of  $B^\pm \rightarrow DK^\pm$  decays, the ADS/GLW analysis of  $B^0 \rightarrow DK^{*0}$  decays and the time-dependent analysis of  $B_s^0 \rightarrow D_s^\mp K^\pm$  decays.

## 1. Introduction

The CKM angle  $\gamma$ , defined as  $\gamma \equiv \arg\left(-\frac{V_{ud}V_{ub}^*}{V_{cd}V_{cb}^*}\right)$ , is the least known CKM parameter. B-factories and the LHCb experiment measured  $\gamma$  with an uncertainty larger than  $10^\circ$  [1, 2, 3]. To compare, global fits like CKMfitter [4] and UTfit [5] obtain an estimation of  $\gamma$  with an error about  $2^\circ$ . This angle is directly measurable through tree processes, without significant loop contribution. Hence the extraction of its value is very clean and has a theoretical relative uncertainty lower than  $10^{-7}$  [6]. Therefore a precise measurement of  $\gamma$  provides an excellent standard candle to check the consistency of the CKM paradigm in the Standard Model and to probe some new physics. The present paper summarises four measurements of  $\gamma$  performed by the LHCb collaboration and presented at the BEACH 2014 conference.

## 2. Time-integrated measurements of $\gamma$

Given its definition,  $\gamma$  is approximately the phase difference between the quark transitions  $b \rightarrow c\bar{u}s$  and  $b \rightarrow u\bar{c}s$  and the interference between these two transitions is sensitive to this angle. The interference is obtained by reconstructing the  $D^0$  and  $\bar{D}^0$  mesons produced in these decays in an identical final state (Fig. 1). In the case of a three body  $D$  meson decay a Dalitz plot analysis can be carried out. This method is called GGSZ [7, 8] and two recent LHCb results are reported in section 2.1. In the case of a two body  $D$  meson<sup>1</sup> decay a counting analysis is developed following the so called GLW [9, 10] or ADS [11, 12] methods. A recent ADS/GLW result from LHCb is presented in section 2.2. All of these methods can be applied to the channels  $B^\pm \rightarrow DK^\pm$  and  $B^0 \rightarrow DK^{*0}$ . Since these  $B$  mesons decays are self-tagged, no time-dependent analysis is required.

<sup>1</sup> in the following  $D$  stands for either a  $D^0$  or a  $\bar{D}^0$  meson.

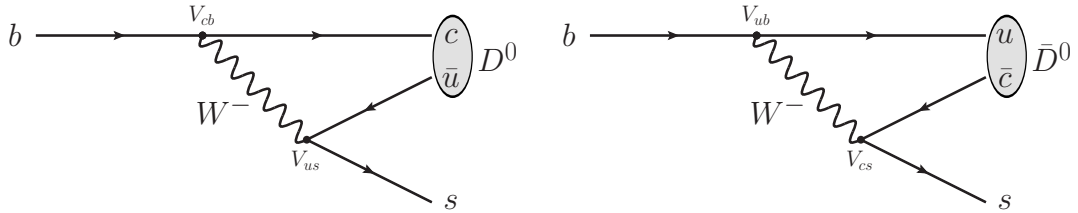


**Figure 1.** Feynman diagrams of  $b \rightarrow c\bar{u}s$  (left) and  $b \rightarrow u\bar{c}s$  (right) decays.

27 *2.1. Measurements with 3-body D meson decays*

The  $B^\pm \rightarrow D(K_S^0 h^+ h^-)K^\pm$  decay amplitude —  $h$  stands for either a charged pion or a charged kaon — can be written as

$$A_{B^\pm}(\mathcal{D}) = A_D(\mathcal{D}) + e^{i(\delta_B \pm \gamma)} A_{\bar{D}}(\mathcal{D}),$$

28 where  $A_D$  ( $A_{\bar{D}}$ ) is the  $D^0$  ( $\bar{D}^0$ ) decay amplitude,  $\mathcal{D}$  represents the  $D$  meson phase space,  $\delta_B$  is the  
 29 strong phase difference and  $\gamma$  is the weak phase difference between the  $D^0$  and  $\bar{D}^0$  channels. The  
 30  $D$  meson phase space is parameterised by two squared invariant masses, for instance  $m^2(K_S^0 \pi^+)$   
 31 and  $m^2(K_S^0 \pi^-)$  on a  $D$  meson Dalitz plot. The sensitivity to  $\gamma$  arises from large asymmetries  
 32 in some region of the Dalitz plot. In order to evaluate  $\gamma$ , the strong phase variation over the  
 33 Dalitz plot must be known. This can be done in two different ways: with a model-dependent  
 34 (MD) method using BaBar’s amplitude model [13], or with a model-independent (MI) method  
 35 using CLEO-c measurements as inputs [14]. Both methods involve fitting the  $D$  meson Dalitz  
 36 plot to extract the polar coordinates  $(r_{B^\pm}, \delta_B, \gamma)$ . The parameter  $r_{B^\pm}$  is the ratio of the  
 37 magnitudes of the suppressed and favoured  $B$  decay amplitudes. The polar coordinates are  
 38 not estimated directly from the Dalitz fit, but the cartesian coordinates  $x_\pm = r_{B^\pm} \cos(\delta_B \pm \gamma)$   
 39 and  $y_\pm = r_{B^\pm} \sin(\delta_B \pm \gamma)$ .

40 *2.1.1. Model-dependent analysis* This section presents the model-dependent analysis of the  
 41  $B^\pm \rightarrow D(K_S^0 \pi^+ \pi^-)K^\pm$  signal, using a sample of proton-proton collision data at a centre-of-  
 42 mass energy of 7 TeV corresponding to an integrated luminosity of  $1 \text{ fb}^{-1}$ . Full details can  
 43 be found in Ref. [15]. The analysis is carried out in two distinct stages. First a fit to the  $B$   
 44 meson reconstructed invariant mass is performed on the selected  $B^\pm \rightarrow D(K_S^0 \pi^+ \pi^-)K^\pm$  and  
 45  $B^\pm \rightarrow D(K_S^0 \pi^+ \pi^-)\pi^\pm$  candidates. This fit determines the signal and background fractions in  
 46 the data sample. A total yield of 637  $B^\pm \rightarrow D(K_S^0 \pi^+ \pi^-)K^\pm$  signal events and 8866 events of  
 47 the  $B^\pm \rightarrow D(K_S^0 \pi^+ \pi^-)\pi^\pm$  control channel are found. Then a fit to the Dalitz plot determines the  
 48  $CP$  violation observables  $(x_\pm, y_\pm)$ . The signal and background yields and the parameters of the  
 49  $B$  invariant mass probability distribution function are fixed to the values obtained in the first  
 50 stage. The model used to describe the amplitude of the  $D^0 \rightarrow K_S^0 \pi^+ \pi^-$  decay over the phase  
 51 space is the one determined by the BaBar collaboration in Ref. [13]. Fitting simultaneously  
 52 the distributions in the  $D^0 \rightarrow K_S^0 \pi^+ \pi^-$  phase space for the  $B^\pm \rightarrow D(K_S^0 \pi^+ \pi^-)K^\pm$  and the  
 53  $B^\pm \rightarrow D(K_S^0 \pi^+ \pi^-)\pi^\pm$  candidates enables to take into account the variation of efficiency over  
 54 the phase space. The  $B^\pm \rightarrow D(K_S^0 \pi^+ \pi^-)\pi^\pm$  decay is a good proxy to get the efficiency variation,  
 55 since it has a kinematic topology similar to the signal one and  $CP$  violation can be neglected in  
 56 this channel. The resulting values of the cartesian coordinates are

$$\begin{aligned} x_- &= +0.027 \pm 0.044_{-0.008}^{+0.010} \pm 0.001, & x_+ &= -0.084 \pm 0.045 \pm 0.009 \pm 0.005, \\ y_- &= +0.013 \pm 0.048_{-0.007}^{+0.009} \pm 0.003, & y_+ &= -0.032 \pm 0.048_{-0.009}^{+0.010} \pm 0.008, \end{aligned}$$

58 where the first uncertainty is statistical, the second systematic and the third due to the amplitude  
59 model used to describe the  $D^0 \rightarrow K_S^0 \pi^+ \pi^-$  decay. The leading experimental systematic errors  
60 are due to the efficiency and background description uncertainties. The constraints obtained on  
61 the polar coordinates are  $r_{B^\pm} = 0.06 \pm 0.04$ ,  $\delta_B = (115_{-51}^{+41})^\circ$  and  $\gamma = (84_{-42}^{+49})^\circ$ . These results are  
62 consistent with those of the LHCb model-independent analysis based on the same data set [16].

*2.1.2. Model-independent analysis* This section presents the model-independent analysis of the  
 $B^\pm \rightarrow D(K_S^0 h^+ h^-) K^\pm$  decays, using a sample of proton-proton collision data at a centre-of-  
mass energy of 7 and 8 TeV corresponding to a total integrated luminosity of  $3 \text{ fb}^{-1}$ . Full details  
can be found in Ref. [17]. There is a significant improvement compared to the former results in  
Ref. [16], thanks to the increased statistics and a better analysis technique. To know the strong  
phase variation over the  $D^0 \rightarrow K_S^0 h^+ h^-$  phase space the measurements made by CLEO-c, in  
a particular binning scheme, is used [14]. In this way the analysis is a counting experiment in  
bins of the Dalitz plot. The expected number of  $D$  from  $B^+$  events falling in a particular bin  
labelled  $\pm i$  (the  $\pm$  sign comes from the phase symmetry with respect to the Dalitz diagonal) can  
be expressed as

$$N_{\pm i}^+ = h_B^+ \left[ F_{\mp i} + (x_+^2 + y_+^2) F_{\pm i} + 2\sqrt{F_i F_{-i}} (x_+ c_{\pm i} \mp y_+ s_{\pm i}) \right], \quad (1)$$

63 where  $c_i$  and  $s_i$  are the averaged cosine and sine of the strong phase difference in bin  $i$  (CLEO-c  
64 inputs),  $F_i$  is the expected fraction of pure  $D^0$  events in bin  $i$  taking into account the efficiency  
65 profile over the phase space, and  $h_B^+$  is a normalisation factor. The  $F_i$  parameters are deter-  
66 mined from the  $B^0 \rightarrow D^{*\pm} \mu^\mp \nu_\mu$  control mode. This is an excellent proxy because the sample  
67 has a high purity, a high statistics and the  $D^0$  meson is tagged thanks to the slow pion in the  
68  $D^{*+} \rightarrow D^0 \pi^+$  decay. Some corrections are applied from simulated data to account for recon-  
69 struction and selection discrepancies between the  $B^0 \rightarrow D^{*\pm} \mu^\mp \nu_\mu$  and the  $B^\pm \rightarrow DK^\pm$  decays.  
70 The fit is performed in two steps. First the phase space integrated  $B^\pm$  mass fit determines the  
71 total signal yields (around 2600) and fixes the model used in the second step. This last fit is  
72 made in each Dalitz bin with all the parameters in Eq. (1) fixed but the normalisation factor  
73 and the  $(x_\pm, y_\pm)$  observables. The resulting values of the cartesian coordinates (Fig. 2) are the  
74 most precise to date:

$$\begin{aligned} x_- &= (2.5 \pm 2.5 \pm 1.0 \pm 0.5) \times 10^{-2}, & x_+ &= (-7.7 \pm 2.4 \pm 1.0 \pm 0.4) \times 10^{-2}, \\ y_- &= (7.5 \pm 2.9 \pm 0.5 \pm 1.4) \times 10^{-2}, & y_+ &= (-2.2 \pm 2.5 \pm 0.4 \pm 1.0) \times 10^{-2}, \end{aligned}$$

76 where the first uncertainty is statistical, the second systematic and the third due to the exper-  
77 imental knowledge of the  $(c_i, s_i)$  parameters. Compared to the  $1 \text{ fb}^{-1}$  measurement [16], the  
78 statistical uncertainty is reduced thanks to the larger data sample, the experimental systematic  
79 is reduced by using the new control mode  $B^0 \rightarrow D^{*\pm} \mu^\mp \nu_\mu$ , and the  $(c_i, s_i)$  systematic is also  
80 improved by the increased LHCb sample size. The results are:  $r_{B^\pm} = 0.080_{-0.021}^{+0.019}$ ,  $\gamma = (62_{-14}^{+15})^\circ$   
81 and  $\delta_B = (62_{-15}^{+14})^\circ$ .

## 82 2.2. Measurements with 2-body $D$ meson decays

This section presents the ADS/GLW analysis of the  $B^0 \rightarrow DK^{*0}$  decays, using a sample of  
proton-proton collision data at a centre-of-mass energy of 7 and 8 TeV corresponding to a  
total integrated luminosity of  $3 \text{ fb}^{-1}$ . Full details can be found in Ref. [18]. Compared to  
the  $B^\pm \rightarrow DK^\pm$  decays, both Cabibbo favoured and suppressed diagrams are color suppressed,  
which brings about a higher interference amplitude ( $r_{B^0}$  is larger than  $r_{B^\pm}$ ). Hence a better  
sensitivity to  $\gamma$  is expected. However this neutral channel is experimentally more challenging.  
For the GLW modes the  $D$  mesons are reconstructed in two  $CP$  eigenstate:  $K^+ K^-$  and  $\pi^+ \pi^-$ .

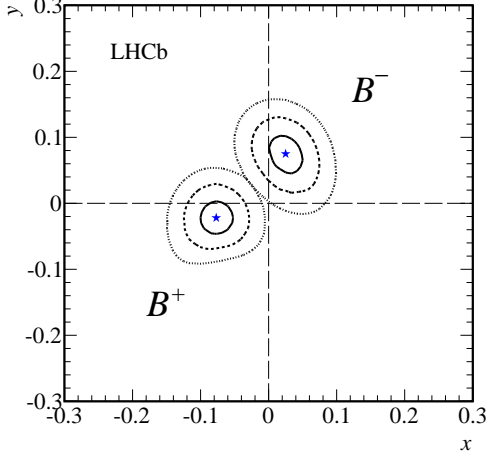


**Figure 2.** Confidence levels at 39.3%, 86.5% and 98.9% probability for  $(x_+, y_+)$  and  $(x_-, y_-)$  as measured in  $B^\pm \rightarrow DK^\pm$  decays (statistical uncertainties only). The parameters  $(x_+, y_+)$  relate to  $B^+$  decays and  $(x_-, y_-)$  refer to  $B^-$  decays. The stars represent the best fit central values.

For the ADS modes the  $D$  mesons are reconstructed in the  $K^+\pi^-$  and  $K^-\pi^+$  final states. From these decays several observables sensitive to  $\gamma$  can be built. For instance in the GLW modes the  $CP$  asymmetries

$$A_d^{hh} \equiv \frac{\Gamma(\bar{B}^0 \rightarrow D(h^+h^-)\bar{K}^{*0}) - \Gamma(B^0 \rightarrow D(h^+h^-)K^{*0})}{\Gamma(\bar{B}^0 \rightarrow D(h^+h^-)\bar{K}^{*0}) + \Gamma(B^0 \rightarrow D(h^+h^-)K^{*0})} = \frac{2r_{B^0}\kappa \sin \delta_B \sin \gamma}{1 + r_{B^0}^2 + 2r_{B^0}\kappa \cos \delta_B \cos \gamma}$$

are measured. The parameter  $\kappa$  is the coherence factor introduced to account for the effect of the non resonant  $B^0 \rightarrow DK^+\pi^-$  contribution in the  $K^{*0}$  signal region. And in the ADS mode the ratio of suppressed  $B^0 \rightarrow D(\pi^+K^-)K^{*0}$  to favoured  $B^0 \rightarrow D(K^+\pi^-)K^{*0}$  partial widths are measured separately for  $B^0$  and  $\bar{B}^0$ :

$$R_d^+ \equiv \frac{\Gamma(B^0 \rightarrow D(\pi^+K^-)K^{*0})}{\Gamma(B^0 \rightarrow D(K^+\pi^-)K^{*0})} = \frac{r_{B^0}^2 + r_D^2 + 2r_{B^0}r_D\kappa \cos(\delta_B + \delta_D + \gamma)}{1 + r_{B^0}^2r_D^2 + 2r_{B^0}r_D\kappa \cos(\delta_B - \delta_D + \gamma)},$$

$$R_d^- \equiv \frac{\Gamma(\bar{B}^0 \rightarrow D(\pi^-K^+)\bar{K}^{*0})}{\Gamma(\bar{B}^0 \rightarrow D(K^-\pi^+)\bar{K}^{*0})} = \frac{r_{B^0}^2 + r_D^2 + 2r_{B^0}r_D\kappa \cos(\delta_B + \delta_D - \gamma)}{1 + r_{B^0}^2r_D^2 + 2r_{B^0}r_D\kappa \cos(\delta_B - \delta_D - \gamma)}.$$

The parameters  $r_D$  and  $\delta_D$  are the magnitude ratio and the phase difference, respectively, between the amplitudes of the  $D^0 \rightarrow K^+\pi^-$  and  $D^0 \rightarrow K^-\pi^+$  decays. The significances of the combined  $B^0$  and  $\bar{B}^0$  signals for the  $B^0 \rightarrow D(K^+K^-)K^{*0}$ ,  $B^0 \rightarrow D(\pi^+\pi^-)K^{*0}$  and  $B^0 \rightarrow D(\pi^+K^-)K^{*0}$  decay modes are  $8.6 \sigma$ ,  $5.8 \sigma$  and  $2.9 \sigma$  respectively. Once the production and efficiency asymmetries are taken into account the results are:

$$A_d^{KK} = -0.20 \pm 0.15 \pm 0.02, \quad R_d^+ = 0.06 \pm 0.03 \pm 0.01,$$

$$A_d^{\pi\pi} = -0.09 \pm 0.22 \pm 0.02, \quad R_d^- = 0.06 \pm 0.03 \pm 0.01,$$

where the first uncertainties are statistical and the second systematic.  $A_d^{\pi\pi}$ ,  $R_d^+$  and  $R_d^-$  are first measurements and the  $A_d^{KK}$  result supersedes the former LHCb one [19]. From these measurements the value of  $r_{B^0}$  (proper to the  $B^0 \rightarrow DK^{*0}$  channel) is found to be  $r_{B^0} = 0.240_{-0.048}^{+0.055}$ . This is the most precise measurement to date.

### 3. Time-dependent measurement of $\gamma$

This section presents the time-dependent analysis of the  $B_s^0 \rightarrow D_s^\mp K^\pm$  decays, using a sample of proton-proton collision data at a centre-of-mass energy of 7 TeV corresponding to an integrated

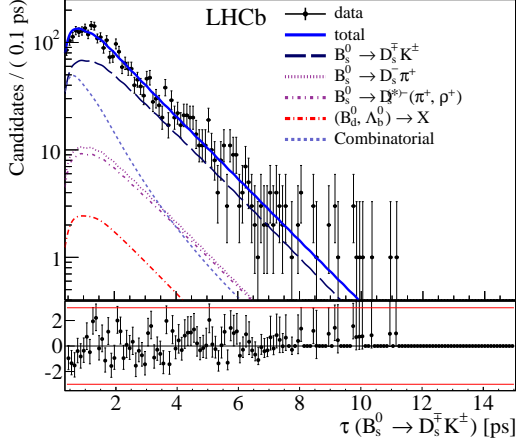


**Figure 3.** Result of the decay-time *cFit* to the  $B_s^0 \rightarrow D_s^\mp K^\pm$  candidates.

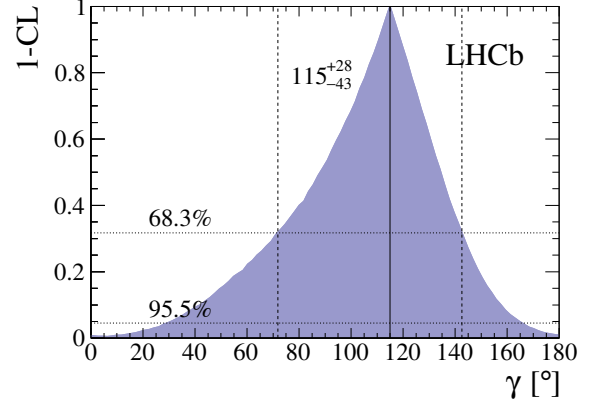


**Figure 4.** Frequentist interpretation of the  $\gamma$  measurement in term of confidence interval.

100 luminosity of  $1 \text{ fb}^{-1}$ . Full details can be found in Ref. [20]. In addition to the same tree level  
 101 processes as in the time-integrated analysis (Fig. 1), the effect of the  $B_s$  mixing occurs. Hence  
 102 the interference between mixing and decay amplitudes in  $B_s^0 \rightarrow D_s^\mp K^\pm$  is sensitive to the  $CP$   
 103 violating phase  $(\gamma - 2\beta_s)$  where  $\beta_s \equiv \arg(-V_{ts}V_{tb}^*/V_{cs}V_{cb}^*)$ . The time-dependent decay rates  
 104 depend on the  $CP$  observables

$$105 \quad C_f = \frac{1-r_{D_s K}^2}{1+r_{D_s K}^2}, \quad A_f^{\Delta\Gamma} = \frac{-2r_{D_s K} \cos(\delta - (\gamma - 2\beta_s))}{1+r_{D_s K}^2}, \quad A_{\bar{f}}^{\Delta\Gamma} = \frac{-2r_{D_s K} \cos(\delta + (\gamma - 2\beta_s))}{1+r_{D_s K}^2},$$

$$S_f = \frac{2r_{D_s K} \sin(\delta - (\gamma - 2\beta_s))}{1+r_{D_s K}^2}, \quad S_{\bar{f}} = \frac{-2r_{D_s K} \sin(\delta + (\gamma - 2\beta_s))}{1+r_{D_s K}^2},$$

106 where  $r_{D_s K}$  is the magnitude of the amplitude ratio  $|A(\bar{B}_s^0 \rightarrow D_s^- K^+)/A(B_s^0 \rightarrow D_s^- K^+)|$ ,  $\delta$   
 107 the strong phase difference and  $(\gamma - 2\beta_s)$  the weak phase difference. This analysis uses an  
 108 independent measurement of  $\phi_s$  [21] and assumes  $\phi_s = -2\beta_s$  to interpret the results in terms  
 109 of  $\gamma$ . To discriminate the signal and background components a 3D fit is performed on the  $B_s$   
 110 and  $D_s$  masses along with the log-likelihood difference between the kaon and pion hypothesis for  
 111 the companion particle ( $K^\pm$  for  $B_s^0 \rightarrow D_s^\mp K^\pm$  signal and  $\pi^+$  for  $B_s^0 \rightarrow D_s^- \pi^+$  control mode).  
 112 Then the output of this multivariate fit is used for the decay-time fit. Two fits are performed: a  
 113 background subtracted fit, called *sFit*, using the *sWeights* [22, 23] determined by the multivariate  
 114 fit; and a classical fit, called *cFit* (Fig. 3) where all signal and background time distributions are  
 115 described. The results of these two fits are in excellent agreement:

Parameter	<i>sFit</i> fitted value	<i>cFit</i> fitted value
$C_f$	$0.52 \pm 0.25 \pm 0.04$	$0.53 \pm 0.25 \pm 0.04$
$A_f^{\Delta\Gamma}$	$0.29 \pm 0.42 \pm 0.17$	$0.37 \pm 0.42 \pm 0.20$
$A_{\bar{f}}^{\Delta\Gamma}$	$0.14 \pm 0.41 \pm 0.18$	$0.20 \pm 0.41 \pm 0.20$
$S_f$	$-0.09 \pm 0.31 \pm 0.06$	$-1.09 \pm 0.33 \pm 0.08$
$S_{\bar{f}}$	$-0.36 \pm 0.34 \pm 0.06$	$-0.36 \pm 0.34 \pm 0.08$

117 The first uncertainties are statistical and the second systematic. The main sources of systematic  
 118 arise from the trigger-induced time-dependent efficiency,  $\Gamma_s$  and  $\Delta\Gamma_s$ . These results can be  
 119 interpreted as a confidence interval  $\gamma = (115_{-43}^{+28})^\circ$  at 68% CL (Fig. 4). This is the first  
 120 measurement of  $\gamma$  with  $B_s^0 \rightarrow D_s^\mp K^\pm$  decays.

## 4. Conclusion

The latest LHCb results on the CKM angle  $\gamma$  are reported: the model dependent GGSZ analysis of  $B^\pm \rightarrow DK^\pm$  decays, the update to the full available data set of the model independent GGSZ analysis of  $B^\pm \rightarrow DK^\pm$  decays, the ADS/GLW analysis of  $B^0 \rightarrow DK^{*0}$  decays and the first  $\gamma$  measurement with  $B_s^0 \rightarrow D_s^\mp K^\pm$  decays. Using these results and the corresponding improvements, the next combination of the LHCb  $\gamma$  measurements should yield a significant reduction of the uncertainty.

## References

- [1] BaBar collaboration, J. P. Lees *et al.*, *Observation of direct CP violation in the measurement of the Cabibbo-Kobayashi-Maskawa angle gamma with  $B^\pm \rightarrow D^{(*)}K^{(*)\pm}$  decays*, Phys. Rev. **D87** (2013), no. 5 052015, [arXiv:1301.1029](#).
- [2] Belle collaboration, K. Trabelsi, *Study of direct CP in charmed B decays and measurement of the CKM angle gamma at Belle*, [arXiv:1301.2033](#).
- [3] LHCb collaboration, *Improved constraints on  $\gamma$  from  $B^\pm \rightarrow DK^\pm$  decays including first results on 2012 data*, Linked to LHCb-ANA-2013-012.
- [4] CKMfitter Group, J. Charles *et al.* Eur. Phys. J. **C41** (2005) 1, [arXiv:hep-ph/0406184](#), updated results and plots available at: <http://ckmfitter.in2p3.fr>.
- [5] UTfit collaboration, M. Bona *et al.* JHEP **0610** (2006) 081, [arXiv:hep-ph/0606167](#), updated results and plots available at: <http://www.utfit.org>.
- [6] J. Brod and J. Zupan, *The ultimate theoretical error on  $\gamma$  from  $B \rightarrow DK$  decays*, JHEP **1401** (2014) 051, [arXiv:1308.5663](#).
- [7] A. Giri, Y. Grossman, A. Soffer, and J. Zupan, *Determining  $\gamma$  using  $B^\pm \rightarrow DK^\pm$  with multibody D decays*, Phys. Rev. D **68** (2003) 054018.
- [8] A. Bondar in *Proceedings of BINP special analysis meeting on Dalitz*, unpublished, 2002.
- [9] M. Gronau and D. London, *How to determine all the angles of the unitarity triangle from  $B_d^0 \rightarrow DK_S$  and  $B_s^0 \rightarrow D\phi$* , Physics Letters B **253** (1991), no. 3-4 483 .
- [10] M. Gronau and D. Wyler, *On determining a weak phase from charged b decay asymmetries*, Physics Letters B **265** (1991), no. 1-2 172 .
- [11] D. Atwood, I. Dunietz, and A. Soni, *Enhanced CP Violation with  $B \rightarrow KD^0(\bar{D}^0)$  Modes and Extraction of the Cabibbo-Kobayashi-Maskawa Angle  $\gamma$* , Phys. Rev. Lett. **78** (1997) 3257.
- [12] D. Atwood, I. Dunietz, and A. Soni, *Improved methods for observing CP violation in  $B^\pm \rightarrow KD$  and measuring the CKM phase  $\gamma$* , Phys. Rev. D **63** (2001) 036005.
- [13] BaBar collaboration, P. del Amo Sanchez *et al.*, *Measurement of  $D^0 - \bar{D}^0$  mixing parameters using  $D^0 \rightarrow K_S^0 \pi^+ \pi^-$  and  $D^0 \rightarrow K_S^0 K^+ K^-$  decays*, Phys. Rev. Lett. **105** (2010) 081803, [arXiv:1004.5053](#).
- [14] CLEO collaboration, J. Libby *et al.*, *Model-independent determination of the strong-phase difference between  $D^0$  and  $\bar{D}^0 \rightarrow K_{S,L}^0 h^+ h^-$  ( $h = \pi, K$ ) and its impact on the measurement of the CKM angle  $\gamma/\phi_3$* , Phys. Rev. **D82** (2010) 112006, [arXiv:1010.2817](#).
- [15] LHCb collaboration, R. Aaij *et al.*, *Measurement of CP violation and constraints on the CKM angle  $\gamma$  in  $B^\pm \rightarrow DK^\pm$  with  $D \rightarrow K_S^0 \pi^+ \pi^-$  decays*, [arXiv:1407.6211](#), submitted to Nucl. Phys. B.
- [16] LHCb collaboration, R. Aaij and other, *A model-independent Dalitz plot analysis of  $B^\pm \rightarrow DK^\pm$  with  $D \rightarrow K_S^0 h^+ h^-$  ( $h = \pi, K$ ) decays and constraints on the CKM angle  $\gamma$* , Phys. Lett. **B718** (2012) 43, [arXiv:1209.5869](#).
- [17] LHCb collaboration, R. Aaij and other, *Measurement of the CKM angle  $\gamma$  using  $B^\pm \rightarrow DK^\pm$  with  $D \rightarrow K_S^0 \pi^+ \pi^-$ ,  $K_S^0 K^+ K^-$  decays*, [arXiv:1408.2748](#), submitted to JHEP.
- [18] LHCb collaboration, R. Aaij and other, *Measurements of CP violation parameters in  $B^0 \rightarrow DK^{*0}$  decays*, [arXiv:1407.8136](#), submitted to Phys. Rev. D.
- [19] LHCb collaboration, R. Aaij and other, *Measurement of CP observables in  $B^0 \rightarrow DK^{*0}$  with  $D \rightarrow K^+ K^-$* , JHEP **03** (2013) 067, [arXiv:1212.5205](#).
- [20] LHCb collaboration, R. Aaij and other, *Measurement of CP asymmetry in  $B_s^0 \rightarrow D_s^\mp K^\pm$  decays*, [arXiv:1407.6127](#), submitted to JHEP.
- [21] LHCb collaboration, R. Aaij and other, *Measurement of CP violation and the  $B_s^0$  meson decay width difference with  $B_s^0 \rightarrow J/\psi K^+ K^-$  and  $B_s^0 \rightarrow J/\psi \pi^+ \pi^-$  decays*, Phys. Rev. **D87** (2013) 112010, [arXiv:1304.2600](#).
- [22] M. Pivk and F. R. Le Diberder, *sPlot: A statistical tool to unfold data distributions*, Nuclear Instruments and Methods in Physics Research A **555** (2005) 356, [arXiv:physics/0402083](#).
- [23] Y. Xie, *sFit: a method for background subtraction in maximum likelihood fit*, ArXiv e-prints (2009) [arXiv:0905.0724](#).